Pramana – J. Phys. (2020) 94:110
https://doi.org/10.1007/s12043-020-01980-3

Amorphisation of boron carbide under gamma irradiation

MATLAB N MIRZAYEV[1,2,*], ERTUĞRUL DEMIR[1,3], KHAGANI F MAMMADOV[2], VLADIMIR A SUKRATOV[1], SAKIN H JABAROV[2,4], SAPHINA BIIRA[5], ELMAR B ASGEROV[1], BEKHZODJON A ABDURAKHIMOV[6] and A BERIL TUĞRUL[3]

[1]Joint Institute for Nuclear Research, Dubna, Moscow Distr., Russia 141980
[2]Institute of Radiation Problems, Azerbaijan National Academy of Sciences, 1143 Baku, Azerbaijan
[3]Istanbul Technical University, 34469 Istanbul, Turkey
[4]Azerbaijan State Pedagogical University, Baku AZ-1000, Azerbaijan
[5]Department of Physics, Busitema University, P.O. Box 236, Tororo, Uganda
[6]Institute of Nuclear Physics, Academy of Sciences of Uzbekistan, 100214 Tashkent, Uzbekistan
*Corresponding author. E-mail: matlab@jinr.ru

MS received 13 August 2019; revised 8 December 2019; accepted 23 April 2020;
published online 21 July 2020

Abstract. Boron carbide (B_4C) has been widely used in nuclear reactors and nuclear applications. In this work, the high-purity (99.9%) B_4C samples were irradiated using a gamma source (^{60}Co) with a dose rate (D) of 0.27 Gy/s at different gamma irradiation doses at room temperature. Phase and microstructural characterisation of B_4C samples were carried out using X-ray diffraction (XRD) and scanning electron microscopy (SEM). XRD results displayed some degradation of the diffraction peaks. The calculations reveal that 62% of B_4C has changed into the amorphous phase when the irradiation dose is 194.4 kGy. Fourier transform infrared spectroscopy (FTIR) was used to explain chemical bonds and functional groups of B_4C samples before and after gamma irradiation. The results showed that C–C chemical bonds are weaker than B–C chemical bonds and tend to break under gamma irradiation. Element mapping analysis for each gamma irradiation dose of B_4C samples was performed using SEM patterns. The dynamics of the elements on the surface and chemical formula of all B_4C samples were also determined after gamma irradiation.

Keywords. Boron carbide; gamma irradiation; amorphisation; scanning electron microscopy; X-ray diffraction; Fourier transform infrared spectroscopy; elemental mapping analysis.

PACS Nos 61.05.cj; 61.05.cp; 71.23.Cp; 07.85.−m; 68.37.Hk; 33.20.Ea

1. Introduction

In recent years, boron ceramic compounds such as BSi_n, B_nC, SiBC, BC-ZrC, ZrB_2 and BSi-ZrC have been widely studied and have attracted considerable interest from researchers [1–6]. Elemental boron forms a wide variety of compounds with electron deficiency and unusual binding states. The number of boron modifications has not been fully understood till now. However, it is well-known that boron has two crystalline modifications under normal pressure, known as α-rhombohedral boron and β-rhombohedral boron [7]. Higher borides are also reasonable candidates for high-temperature applications in the technology due to their large Seebeck coefficients and intrinsic low thermal conductivity [8,9]. Boron carbide, commonly referred to as B_4C, has an enigmatic ability to adapt to major changes in carbon composition (up to $B_{10}C$) without any fundamental structural change. B_4C is one of the most studied material among the carbonaceous compounds due to its unique physical and chemical properties [10,11]. However, major aspects of the bond in B_4C and the significant structural changes caused by changing the carbon concentration are still not clearly comprehended [12]. On the other hand, B_4C is widely used for producing ballistic armor [13] and neutron detectors [14,15]. B_4C possesses a combination of outstanding features in material science such as high-melting temperature properties and perfect crystal structure geometry [16–19]. Due to its degree of special rigidity and good mechanical properties, B_4C is in some cases included in the composition of materials that require very high resistance to different chemical mixtures [20–23]. Therefore, it is widely used in the fields of advanced technology. B_4C is used

in nuclear technology for producing of neutron absorbing materials [9,24]. It is used in almost any type of nuclear power plant due to its high neutron absorption efficiency, easy availability and relatively low cost. Its electrical and thermomechanical properties are due to the interatomic bonding, which is essentially covalent. However, its poor thermomechanical properties, when used as a neutron absorber, lead to damage and a short life cycle. Two main events occur in the nuclear reactors. First, atomic displacements cause high point defects, resulting in structural issues in nuclear reactor materials. Amorphisation is one such issue. Secondly, helium production causes damage to microstructural stability [25]. Studies on the irradiation of B_4C with heavy ions at different doses revealed some structural changes in these compounds [26–28]. Most of the processes under the influence of various ionising radiation have shown some degradation in its crystal structure [29]. However, it is capable of self-healing and recombination of radiation defects after a low and high irradiation dose [30–33]. Icosahedral boron-rich solids are materials that contain boron-rich units where atoms are located in 12 corners of an icosahedron. These materials are well known for their extraordinary bonding and unusual structures. The studies clarify that this self-healing is of unusual structural and electronic stability of boron-rich icosahedra fragments [34,35]. Amorphisation is characterised by changes in the structural parameters of the materials that alter the physical and chemical properties of the compound [36,37]. Some studies have been carried out to better understand the amorphisation behaviour of B_4C under irradiation conditions. Regarding the irradiation of B_4C with electrons, an amorphous structure was observed in the irradiation with 2 MeV electrons at low temperatures. On the contrary, there was no amorphous phase for 1 MeV electron irradiation at room temperature [38,39]. It has also been shown that B_4C has a very high structural stability under irradiation conditions, which is much higher than indicated when compared to similar compounds such as silicon carbide [40,41]. In the literature review, we could not find any study about structural parameters, especially amorphisation of B_4C compounds under gamma irradiation conditions. Therefore, in this study, we aimed to investigate the effects of gamma irradiation on microstructure, especially amorphisation of B_4C compounds.

2. Experimental

Boron carbide (B_4C) samples with a bulk density of 1.8 g/cm^3, specific surface area of 2–4 m^2/g, particle size of 1–10 μm and a purity of 99.9% (US Research Nanomaterials, Inc., TX, USA) were used in the experiments. B_4C samples were irradiated using a gamma source (^{60}Co) with a dose rate (D) of 0.27 Gy/s at 9.7, 48.6, 97.2, 145.8 and 194.4 kGy doses at room temperature. The calculated values of the absorbed dose of dosimetric (ferrous sulphate, cyclohexane) system based on the electron density were in agreement with the experimental data [42–46]. Powder samples of B_4C were prepared from single-crystal B_4C and analysed using X-ray diffraction spectra (XRD) at the following parameters: 40 kV, 40 mA, Cu Kα radiation ($\lambda = 1.5406$ Å). The X-ray diffraction spectra were analysed by the Rietveld method using the Fullprof program [47]. The crystalline structures were obtained in the Diamond program [48]. The functional groups and chemical bonds of the irradiated B_4C samples were investigated by Fourier transform infrared (FTIR) spectroscopy (FTIR Varian-640). In order to examine the structural changes in B_4C samples caused by gamma radiation, we used the FTIR spectroscopy method based on the measured spectra of translucent compressed tablets. These tablets were measured by mixing (1:300) B_4C using KBr, under $6 \cdot 10^4$ N/m^2 pressure at room temperature in thin layers of 3–7 μm thickness and $8 \times 30\,mm^2$ sizes in the range of 4000–500 cm^{-1}. The surface morphology and element mapping of B_4C samples were carried out at room temperature using scanning electron microscope (SEM)/ HE-SE2 detector (ZEISS, ΣIGMA VP). It was also used to investigate particle size and microstructural properties of B_4C samples in the experiments, which was performed under vacuum condition of 10^{-7} Pa generated by turbo-molecular pumps [49].

3. Results and discussion

XRD analysis was performed in the range of $15^o < 2\theta < 60^o$ to comprehend the amorphisation kinetics of gamma-irradiated boron samples. The XRD patterns of B_4C before and after gamma irradiation are shown for each gamma dose in figure 1. According to the diffraction pattern of B_4C samples, it has R-3m spatial symmetry group. This finding is consistent with the previous studies [16,17,21]. The lattice parameters of B_4C in ambient conditions were determined as $a = 5.630(2)$ Å and $c = 12.151(4)$ Å at room temperature. The effect of gamma irradiation on the crystalline structure of B_4C was examined by XRD technique before and after irradiation as shown in figure 1a. Furthermore, it can be seen that an increase in gamma irradiation dose of B_4C causes the expansion of diffraction peaks and modifies the formation of the XRD pattern. Moreover, it can also be clearly seen that peak intensities decrease with increasing doses of gamma radiation. Figure 1b shows the

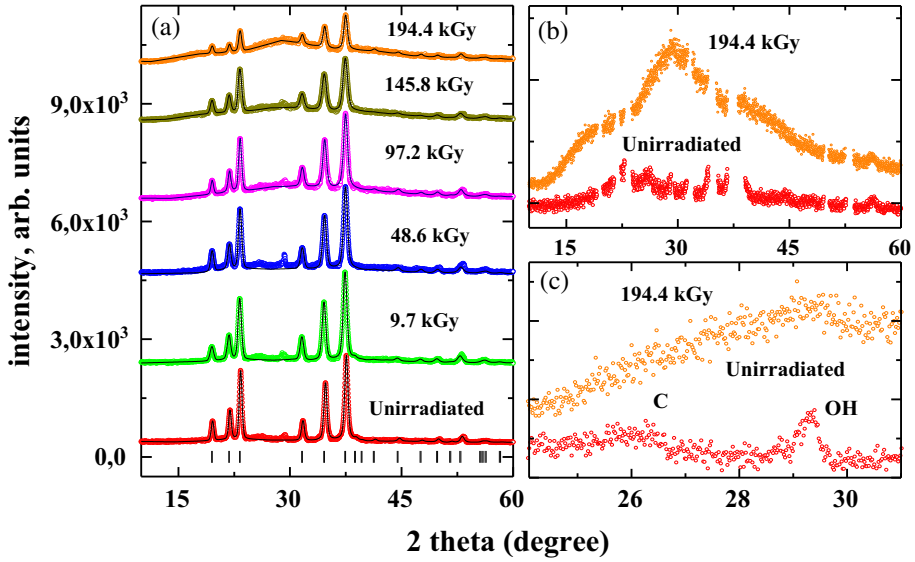

Figure 1. (**a**) XRD spectra of B_4C samples for each gamma irradiation dose, (**b**) the background of XRD spectra for unirradiatied and 194.4 kGy gamma-irradiated B_4C sample and (**c**) XRD spectra of unirradiated and irradiated B_4C samples (194.4 kGy dose) for graphite and hydroxyl group.

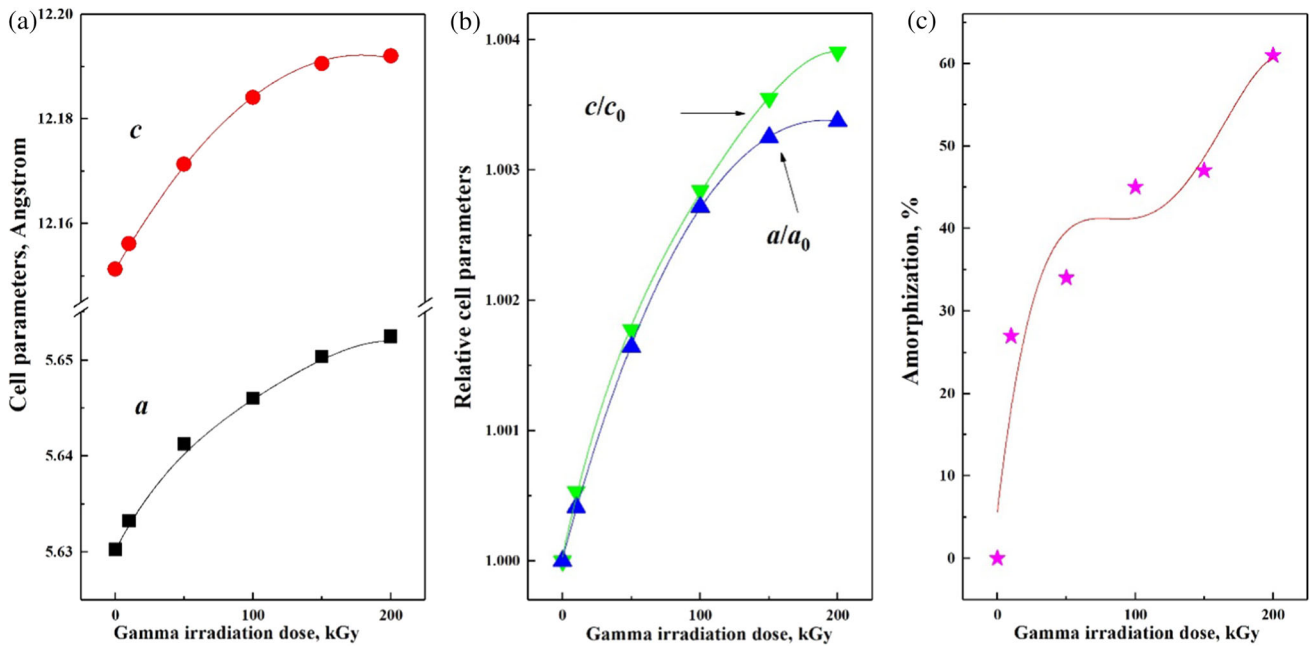

Figure 2. (**a**) The lattice parameters of B_4C samples with increasing gamma irradiation dose, (**b**) a/a_0 and c/c_0 relative values of the lattice parameters depending on gamma irradiation dose and (**c**) amorphisation of B_4C depending on gamma irradiation dose.

background of the XRD spectra to illustrate the amorphisation of the irradiated B_4C samples (at 194.4 kGy). Figure 1b shows that there are strong changes in the background of XRD spectra for 194.4 kGy irradiation dose. This result can be expressed as the degradation of the crystal order of the material and the transition to an amorphous structure. When the material is in amorphous phase, diffraction peaks appear as large lumps distributed over a wide range rather than as narrower peaks of high intensity [50]. On the other hand, as can be seen from figure 1a, a complete amorphous phase does not occur and the diffraction peaks do not completely disappear. Our experimental calculations reveal that 62% of B_4C has changed into the amorphous phase when the irradiation dose is 194.4 kGy. According to the literature review, the diffraction peaks of unirradiated

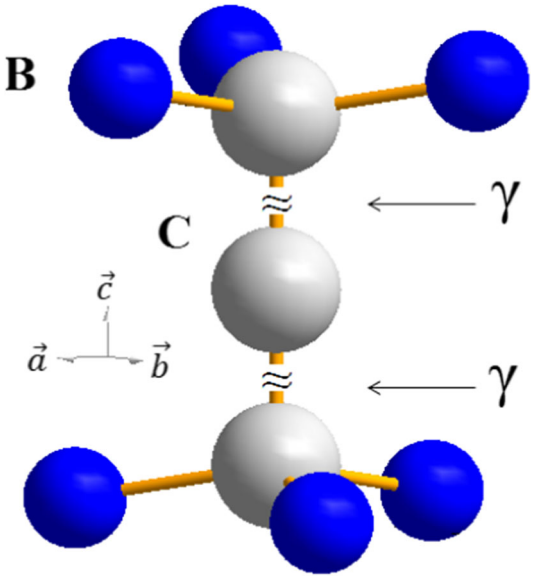

Figure 3. C–C and B–C chemical bonds of B_4C compound.

B_4C samples can be attributed to graphite and B–OH groups (see figure 1c) [51–53]. Conversely, it can be seen that there is almost no hydroxide peak (B–OH) at the 194.4 kGy gamma irradiation dose. The lattice parameters of B_4C were determined as $a = 5.630(2)$ Å and $c = 12.151(4)$ Å at room temperature. Figure 2a shows the change in lattice parameters of B_4C samples with increasing dose of gamma irradiation. A slight increase was detected in the lattice parameters of B_4C samples by gamma irradiation. It is thought that this increase may be due to the breaking of interatomic bonds due to gamma irradiation. The lattice parameter a of B_4C samples as a function of gamma irradiation dose increases by 0.39% which is more than the increase in the value of lattice parameter a (0.33%). The changes of lattice parameters of B_4C samples depending on gamma irradiation dose can be understood clearly from figure 2b. The percentage of amorphisation of B_4C samples was determined using the background field integration method of X-ray diffraction models. Amorphisation of B_4C increased significantly under gamma irradiation up to 97.2 kGy. A slight increase in amorphisation of B_4C was also observed from 97.2 kGy to 145.8 kGy. The results showed that the amorphisation of B_4C samples has reached upto 62% for the maximum irradiation dose (194.4 kGy). The crystal structure of B_4C consists of six boron and three carbon atoms (figure 3). It can be seen that carbon atoms form C–C chemical bonds along the axis $\vec{c}$. On the other hand, B–C chemical bonds were formed in the direction of axes $\vec{a}$ and $\vec{b}$. It is understood from the dependence of the lattice parameters on the gamma absorption dose (figure 2a) that the lattice parameter c changes faster than lattice parameter a under the effect of gamma irradiation. The C–C chemical bonds along the $\vec{c}$-axis are weaker than the B–C chemical bonds and tend to break under gamma irradiation. FTIR spectroscopy was carried out to understand the behaviour of chemical bonds and functional groups of B_4C samples before and after gamma irradiation. FTIR transmission spectra for B_4C at different gamma

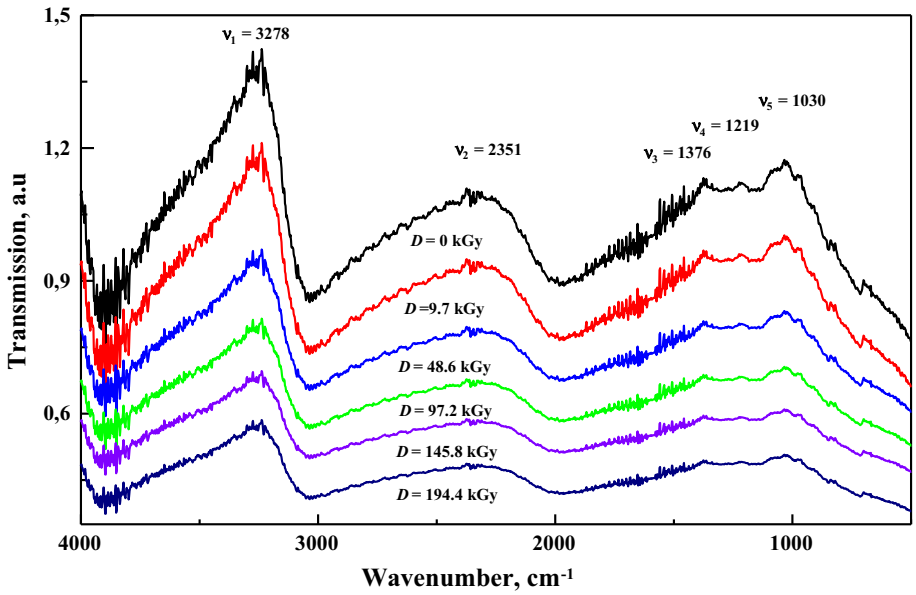

Figure 4. FTIR transmission spectra at different gamma irradiation doses for B_4C samples.

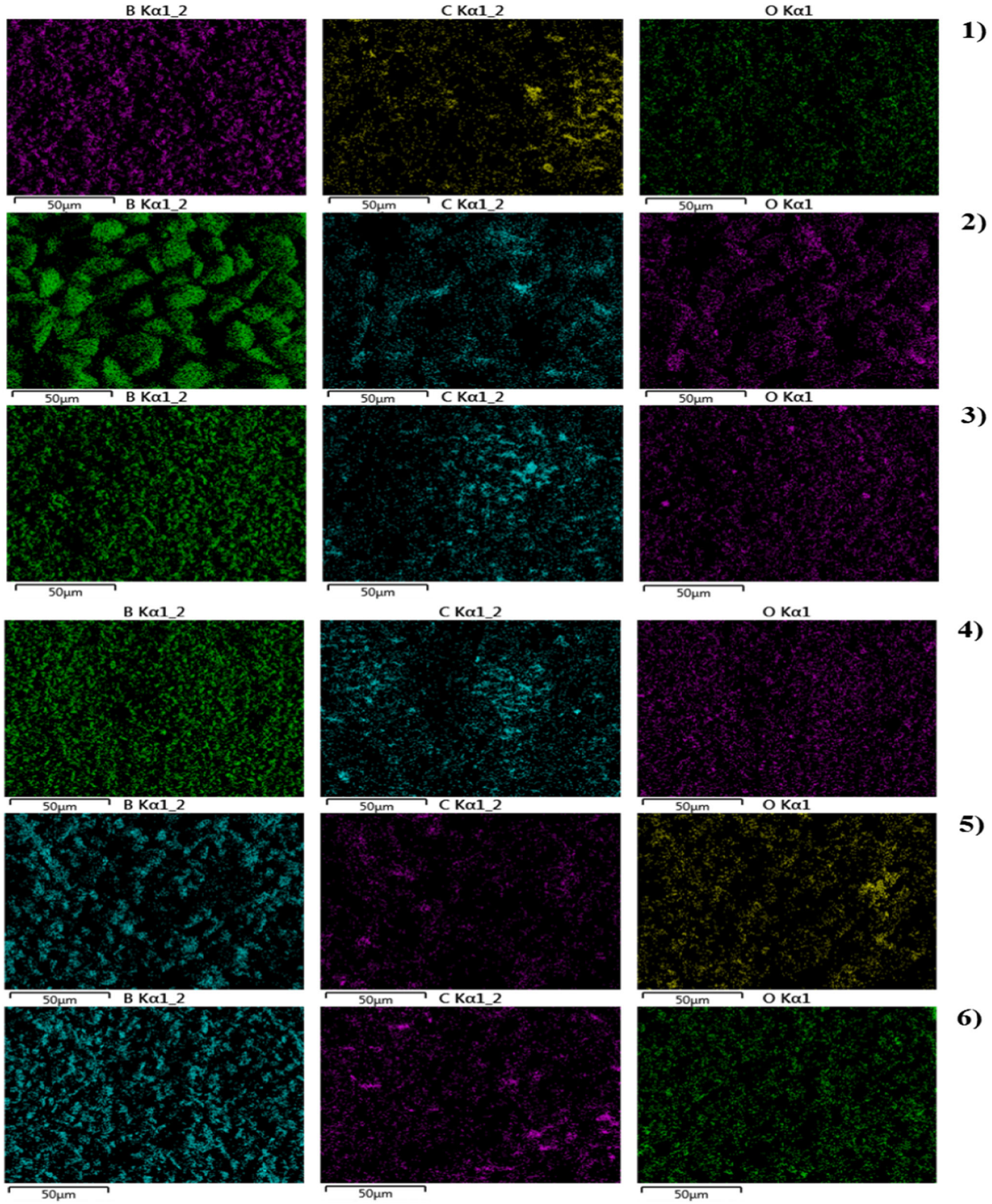

Figure 5. Elemental mapping analysis showing the distributions of B, C and O for (**1**) unirradiated, (**2**) 9.7 kGy, (**3**) 48.6 kGy, (**4**) 97.2 kGy, (**5**) 145.8 kGy and (**6**) 194.4 kGy gamma-irradiated B_4C samples.

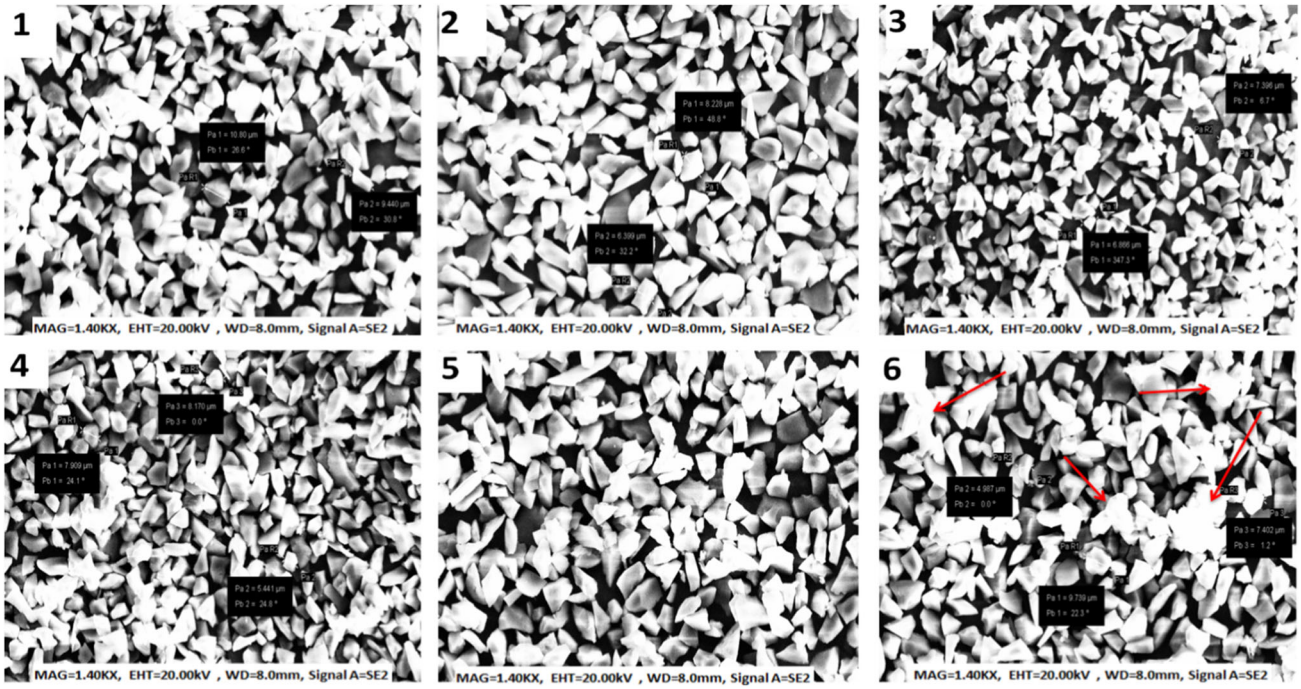

Figure 6. SEM images of (**1**) unirradiated, (**2**) 9.7 kGy, (**3**) 48.6 kGy, (**4**) 97.2 kGy, (**5**) 145.8 kGy and (**6**) 194.4 kGy gamma-irradiated B_4C samples.

absorption doses are seen in figure 4. According to FTIR analysis, the chemical bonds and functional groups of B_4C were determined at $\nu_5 = 1030$, $\nu_4 = 1219$, $\nu_3 = 1376$, $\nu_2 = 2351$ and $\nu_1 = 3278$ cm^{-1}. These peaks can be attributed to B–C, C–O, B–O, C–H, C–OH and B–OH, respectively [54,55]. The presence of hydroxyl groups in the FTIR analysis may be explained by the fact that B_4C powders naturally have the ability to absorb water vapour [56–58]. After high gamma irradiation, the assessment of the physical and chemical processes of the materials is called solvothermal chemical reactions, and this is a very complex process. The concentration of H and OH groups at the surface of the material decreases with increasing dose of gamma radiation. The increase in the temperature of the gamma-irradiated B_4C samples can be explained as the cause of this situation. In our study, the temperature of the materials measured by a thermocouple was approximately 150°C for 194.4 kGy. At this temperature, no OH functional group remained in the material. The following mechanism describes this process:

$$\gamma \xrightarrow{\text{Gamma irradiation}} \text{HOH} \rightarrow \text{H}^* + \text{OH}.$$

Hydrogen atoms and the hydroxyl groups that have emerged after gamma irradiation, are captured by structural defects, excited boron atoms, free carbon atoms and active centres. Moreover, more complex events also occur for hydrogen atoms, hydroxyl groups, carbon and boron atoms. Some of these events are shown as follows:

$$\text{C}^* + \text{H}^* \rightarrow \text{CH}$$

$$\text{OH}^* + \text{OH}^* \rightarrow \text{HOH} + \text{O}$$

$$\text{OH}^* + \text{C}^* \rightarrow \text{C} - [\text{OH}]$$

$$\text{OH}^* + \text{B}^* \rightarrow \text{B} - [\text{OH}].$$

Figure 4 shows that the intensity of the peaks characterising OH groups (B–C and C–H bonds) is decreased by the increase in the gamma radiation dose. OH and C–H groups leave from the structure as vapour afterwards. B_4C bonds break and become amorphous. FTIR analysis revealed that B–OH, B–O and C–O chemical bonds (at 1700, 1389 and 1200 cm^{-1}, respectively) are completely degraded with increasing gamma radiation dose. Furthermore, radical oxygen atoms turned into molecular oxygen, which is also justified by an increase of 0.92% of oxygen in elemental mapping analysis. It can be said that FTIR analysis results are compatible with XRD and SEM results.

Element mapping analysis was performed in B_4C samples of 50 μm cross-section at different doses of gamma radiation as shown in figure 5. Fluctuation dynamics of the elements on the surface of all B_4C samples were determined. The distributions of the B,

C and O elements on the surface of B_4C samples for different gamma irradiation doses are shown in different colours. The results revealed that the distributions of B, C and O elements were not homogeneous on the surface. On the other hand, the distribution of boron elements on the surface was more homogeneous than carbon and oxygen. Moreover, the distribution of B on the surface is much richer than the distribution of C and O. On the other hand, small percentages of Si, Ca, Mg and Al was also found on the surface of B_4C samples. In addition, it has also been reported to be technically difficult to completely remove these elements during the synthesis of B_4C samples. HE-SE2 detector was used to determine the chemical structure of the irradiated materials. The results reveal the chemical formula of gamma-irradiated B_4C samples. $B_{79.1\pm0.4}C_{20.3\pm0.4}O_{0.6\pm0.1}$; $B_{79.3\pm0.4}C_{20.1\pm0.3}O_{0.6\pm0.1}$; $B_{78.6\pm0.4}C_{20.7\pm0.3}O_{0.7\pm0.1}$; $B_{78.9\pm0.4}C_{20.3\pm0.3}O_{0.8\pm0.1}$; $B_{78.3\pm0.4}C_{20.8\pm0.4}O_{0.9\pm0.1}$ and $B_{78.1\pm0.4}C_{20.7\pm0.4}O_{1.2\pm0.1}$ for 9.7, 48.6, 97.2, 145.8, 194.4 kGy, respectively. As can be seen in figure 5, although there is some homogeneity in the distribution of B, it is not the case for C. Furthermore, although B_4C has a high degree of purity, it can be concluded that the emergence of O in the analyses after gamma irradiation is due to the chemical reactions. The results of the elemental mapping analysis have also confirmed that the oxygen atoms on the surface is increased by 0.92%. SEM images of all B_4C samples are shown in figure 6. It should be noted that the SEM images of the B_4C samples were not taken during the gamma irradiation. All measurements were performed at room temperature after irradiation. As can be seen from figure 6, degradations were observed on the surface of the 194.4 kGy gamma-irradiated B_4C samples. The occurrence of amorphisation of B_4C was seen when the gamma irradiation dose was 194.4 kGy. It can be seen as white clouds which are indicated by red arrows in figure 6. The size of the white cloud was measured to be 14–23 μm while the particle size of B_4C was 7–10 μm initially.

4. Conclusion

The process of amorphisation of B_4C samples has been evaluated using ^{60}Co gamma radioisotope ($D = 0.27$ Gy/s) for different gamma irradiation doses at room temperature. X-ray diffraction (XRD), scanning electron microscope (SEM) and Fourier transform infrared spectroscopy (FTIR) analysis were carried out to understand the behaviour of B_4C samples against gamma irradiation. XRD results revelated that lattice parameters of the samples slightly increase with increasing gamma irradiation dose. However, the intensities and expansion of diffraction peaks of B_4C samples decrease with increasing doses of gamma irradiation. Furthermore, XRD results showed that 62% of B_4C has passed into the amorphous phase when the irradiation dose is 194.4 kGy. Under FTIR analysis chemical bonds and functional groups were observed around $\nu_5 = 1030$, $\nu_4 = 1219$, $\nu_3 = 1376$, $\nu_2 = 2351$ and $\nu_1 = 3278$ cm^{-1}. These peaks are respectively assigned to B=C, C=O, B=O, C=H, C=OH and B=OH chemical bonds. In addition, B=OH, B=O and C=O chemical bonds in 1700, 1389 and 1200 cm^{-1} were completely degraded by increasing gamma irradiation dose. The amorphous cluster sizes were observed to be 14–23 μm after gamma irradiation. In contrast, the initial particle size of B_4C was 7–10 μm. The degradation behaviours of chemical bonds and hydroxyl groups of B_4C were examined carefully under gamma irradiation conditions. In this study, the crystal structure and surface morphology of B_4C were studied in detail before and after gamma irradiation. The results show that the amorphisation mechanism of the gamma-irradiated B_4C samples increases depending on the gamma irradiation dose.

Acknowledgements

The corresponding author would like to express his gratitude to the Presidium of Azerbaijan National Academy of Sciences and Science Fund of State Oil Company of the Azerbaijan Republic. Authors also gratefully acknowledge the Flerov Laboratory of Nuclear Reactions of the Joint Institute for Nuclear Research.

References

[1] S Corradetti, S Carturan, L Biasetto, A Andrighetto and P Colombo, *J. Nucl. Mater.* (2013), https://doi.org/10.1016/j.jnucmat.2012.08.024
[2] M Steinbrück, *J. Nucl. Mater.* (2005), https://doi.org/10.1016/j.jnucmat.2004.09.022
[3] M K Aghajanian, B N Morgan, J R Singh, J Mears and R A Wolffe, *Ceram. Trans.* **134**, 527 (2002)
[4] M Shahedi Asl, M Ghassemi Kakroudi and B Nayebi, *Ceram. Int.* (2015), https://doi.org/10.1016/j.ceramint.2014.08.081
[5] D Mallick *et al, Ceram. Int.* (2009), https://doi.org/10.1016/j.ceramint.2008.07.015
[6] C García-Rosales, E Gauthier, J Roth, R Schwörer and W Eckstein, *J. Nucl. Mater.* (1992) https://doi.org/10.1016/0022-3115(92)90413-F
[7] B Albert and H Hillebrecht, *Ang. Chem. Int. Ed.* (2009), https://doi.org/10.1002/anie.200903246
[8] T Mori, *JOM* (2016), https://doi.org/10.1007/s11837-016-2069-9

[9] T Mori and T Nishimura, *J. Solid State Chem.* (2006), https://doi.org/10.1016/j.jssc.2006.03.030
[10] J R Weeks, *Nucl. Sci. Eng.* (2017), https://doi.org/10.13182/nse63-a26270
[11] V Domnich, S Reynaud, R A Habe and M Chhowalla, *J. Am. Ceram. Soc.* (2011), https://doi.org/10.1111/j.1551-2916.2011.04865.x
[12] M M Balakrishnarajan, P D Pancharatna and R Hoffmann, *New J. Chem.* (2007), https://doi.org/10.1039/b618493f
[13] L Desgranges *et al, Nucl. Instrum. Meth. B* (2018), https://doi.org/10.1016/j.nimb.2018.07.011
[14] W A Gooch, *An overview of ceramic armor applications*, 6th Technical conference (Trencin Slovakia, 2004)
[15] D S McGregor, R T Klann, H K Gersch and J D Sanders, *IEEE Nucl. Sci. Symp. Med. Imaging Conf.* (2002), https://doi.org/10.1109/NSSMIC.2001.1009315
[16] D S McGregor, R T Klann, H K Gersch and Y H Yang, *Nucl. Instrum. Meth. Phys. Res. A* (2001), https://doi.org/10.1016/S0168-9002(01)00835-X
[17] T L Aselage, S S McCready and D Emin, *Phys. Rev. B* (2001), https://doi.org/10.1103/PhysRevB.64.054302
[18] F W Glaser, D Moskowitz and B Post, *J. Appl. Phys.* (1953), https://doi.org/10.1063/1.1721367
[19] S K Singh, M Neek-Amal, S Costamagna and F M Peeters, *Phys. Rev. B* (2013), https://doi.org/10.1103/PhysRevB.87.184106
[20] E A Ekimov, V A Sidorov, N N Mel'nik, S Gierlotka and A Presz, *J. Mater. Sci.* (2004), https://doi.org/10.1023/b:jmsc.0000035345.99616.24
[21] F Thévenot, *J. Eur. Ceram. Soc.* (1990), https://doi.org/10.1016/0955-2219(90)90048-K
[22] T Wang and A Yamaguchi, *J. Mater. Sci. Lett.* (2000), https://doi.org/10.1023/A:1006791004355
[23] H E Çamurlu, N Sevinç and Y Topkaya, *J. Mater. Sci.* (2006), https://doi.org/10.1007/s10853-006-0339-6
[24] K Rasim *et al, Angew. Chem. Int. Ed.* (2018), https://doi.org/10.1002/anie.201800804
[25] J O Stiegler and L K Mansur, *Annu. Rev. Mater. Sci.* (2003), https://doi.org/10.1146/annurev.ms.09.080179.002201
[26] D Gosset, S Miro, S Doriot and N Moncoffre, *J. Nucl. Mater.* (2016), https://doi.org/10.1016/j.jnucmat.2016.04.030
[27] D Gosset, S Miro, S Doriot, G Victor and V Motte, *Nucl. Instrum. Meth. Phys. Res. B* (2015), https://doi.org/10.1016/j.nimb.2015.07.054
[28] R E Stoller *et al*, *Nucl. Instrum. Meth. Phys. Res. B* (2013), https://doi.org/10.1016/j.nimb.2013.05.008
[29] G Victor *et al*, *Nucl. Instrum. Meth. Phys. Res. B* (2015), https://doi.org/10.1016/j.nimb.2015.07.082
[30] X Cao *et al*, *Ceram. Int.* (2015), https://doi.org/10.1016/j.ceramint.2014.09.111
[31] S Wu, L Cheng, L Zhang and Y Xu, *Surf. Coatings Technol.* (2006), https://doi.org/10.1016/j.surfcoat.2005.03.009
[32] K Schnarr and H Münzel, *J. Nucl. Mater.* (1990), https://doi.org/10.1016/0022-3115(90)90296-Y
[33] A H Silver and P J Bray, *J. Chem. Phys.* (1958), https://doi.org/10.1063/1.1744697
[34] M Carrard, D Emin and L Zuppiroli, *Phys. Rev. B* (1995), https://doi.org/10.1103/PhysRevB.51.11270
[35] D Emin, *J. Solid State Chem.* (2006), https://doi.org/10.1016/j.jssc.2006.01.014
[36] V Heera *et al*, *Appl. Phys. Lett.* (1997), https://doi.org/10.1063/1.119223
[37] D J Sprouster *et al*, *Phys. Rev. B* (2010), https://doi.org/10.1103/PhysRevB.81.155414
[38] H Inui, H Mori and H Fujita, *Philos. Mag. B* (1990), https://doi.org/10.1080/13642819008208655
[39] T Stoto, N Housseau, L Zuppiroli and B Kryger, *J. Appl. Phys.* (1990), https://doi.org/10.1063/1.346370
[40] E A Kotomin and A I Popov, *Nucl. Instrum. Meth. Phys. Res. B* (1998), https://doi.org/10.1016/S0168-583X(98)00079-2
[41] W J Weber, L M Wang, N Yu and N J Hess, *Mater. Sci. Eng. A* (1998), https://doi.org/10.1016/s0921-5093(98)00710-2
[42] M N Mirzayev *et al*, *J. Alloys Compd.* (2019), https://doi.org/10.1016/j.jallcom.2019.06.135
[43] M Mirzayev *et al*, *Int. J. Mod. Phys. B* **33**, 1950073 (2019)
[44] M N Mirzayev, R N Mehdiyeva, Kh F Mammadov, S H Jabarov and E B Asgerov, *Phys. Part. Nucl. Lett.* **15**, 673 (2018)
[45] M N Mirzayev, S H Jabarov, E B Asgerov, R N Mehdiyeva, T T Thabethe, S Biira and N V Tiep, *Results Phys.* **10**, 541 (2018)
[46] M N Mirzayev, K F Mammadov, R G Garibov and E B Askerov, *High Temp.* **56**, 374 (2018)
[47] J Rodriguez-Carvajal, *Physica B* **192**, 55 (1993)
[48] F Heidelbach, C Riekel and H R Wenk, *J. Appl. Crystallogr.* (1999), https://doi.org/10.1107/S0021889899004999
[49] M N Mirzayev, R N Mehdiyeva, R G Garibov, N A Ismayilova and S Jabarov, *Mod. Phys. Lett. B* **32**, 1850151 (2018)
[50] J Als-Nielsen and Des McMorrow, *Elements of modern X-ray physics* 2nd edn (John Wiley & Sons, 2011), https://doi.org/10.1002/9781119998365
[51] A Mishra, R K Sahoo, S K Singh and B K Mishra, *J. Asian Ceram. Soc.* (2015), https://doi.org/10.1016/j.jascer.2015.08.004
[52] S A Khorrami *et al*, *J. Appl. Chem. Res.* **10**(**4**), 7 (2016)
[53] Q J Guo *et al*, *AIP Adv.* (2018), https://doi.org/10.1063/1.5011782
[54] J Romanos *et al*, *Carbon* (2013), https://doi.org/10.1016/j.carbon.2012.11.031
[55] D Xu *et al*, *Nucl. Instrum. Meth. Phys. Res. B* (1993), https://doi.org/10.1016/0168-583X(93)90737-Q
[56] A Jain and S Anthonysamy, *J. Therm. Anal. Calorim.* (2015), https://doi.org/10.1007/s10973-015-4818-3
[57] Y Z Zheng *et al*, *Chem. Mater.* (2011), https://doi.org/10.1021/cm101525p
[58] https://inis.iaea.org/collection/NCLCollectionStore/_Public/28/023/28023731.pdf